

§7 Numerical Simulation of FRDC-DC Measurement

7. 1. Introduction

The SJTCs show frequency independent ac-dc transfer differences of a few parts in 10^6 . There are two well-known thermoelectric effects that contribute to the ac-dc transfer difference at the 10^{-6} level. One is the second-order Thomson effect along the heater and the other is the Peltier effect at the heater / heater support-lead junctions. In addition to these, local enhancement in Thomson or Peltier coefficients of the heater may occur during manufacturing when the glass-beads are formed by flaming or mechanical stress in the wire.

The thermoelectric effects from different origins and at different locations along the heater are expected to have different characteristic time-constants. For example, thermoelectric effects in the vicinity of the bead may have smaller time-constants compared with the thermoelectric effects at the heater/ heater support junctions. Hence, the characteristic time-constants of the thermoelectric effects may give us a clue for the investigation of the location and the origin of the thermoelectric effects. In this section, a numerical simulation is performed on an SJTC to determine the thermoelectric time-constants due to several possible origins of the thermoelectric effects.

In the previous chapter, a formula which characterizes the frequency-dependence of the FRDC-DC difference of a thermal converter has been derived. The formula was derived using a simple mathematical assumption that the thermoelectric effects develop exponentially with a time-constant τ_{TE} . Validity of this assumption will also be examined using the numerical simulation.

7. 2. Heat transfer equation

When current $I(t)$ is applied to the heater of the SJTC with cross-sectional area A , the temperature distribution of the heater $\theta(x)$ due to the Joule heat and the Thomson effect is determined by a second-order differential equation [7]

$$AC_v \frac{\partial \theta}{\partial t} = \frac{I^2 \rho}{A} + Ak \frac{\partial^2 \theta}{\partial x^2} + \sigma I \frac{\partial \theta}{\partial x} \quad (7.1)$$

where the symbols C_v , k , ρ , and σ represent thermal capacity, thermal conductivity, electric resistivity, and Thomson voltage coefficient of the heater material, respectively.

The temperature distribution of the Joule-heat is slightly modified by non-Joule heating or cooling due to Thomson or Peltier effect. Since the amount of non-Joule heating caused by the thermoelectric effects is more than two orders of magnitude smaller than that of the Joule-heating, the thermoelectric effects were treated as perturbations in the

evaluation of (7.1).

The temperature distribution $\theta(x)$ can be obtained numerically by approximating the differential equation by a step-equation:

$$\begin{aligned} \theta(n;t + \Delta t) &= \theta(n;t) + \frac{\Delta Q_{Total}(n;t)}{\Delta C_v(n)} \times \Delta t \\ \Delta C_v(n) &= C_v(n)A(n)\Delta x(n) \\ \Delta Q_{Total}(n;t) &= \Delta Q_{Joule}(n;t) + \Delta Q_{Conduct}(n;t) + \Delta Q_{Thomson}(n;t) \\ &\quad + \Delta Q_{Peltier}(n;t) + \Delta Q_{Couple}(n;t) \end{aligned} \quad (7.2)$$

where the quantities ΔQ_{xxx} are given by;

$$\begin{aligned} \Delta Q_{Joule}(n;t) &= \rho(n)I^2(t)\Delta x(n)/A(n) \\ \Delta Q_{Conduct}(n;t) &= \left(\frac{kA}{\Delta x}\right)_{n,n+1} [\theta(n+1;t) - \theta(n;t)] \\ &\quad + \left(\frac{kA}{\Delta x}\right)_{n,n-1} [\theta(n-1;t) - \theta(n;t)] \\ \Delta Q_{Thomson}(n;t) &= -\sigma(n)I(t)[\theta(n+1;t) - \theta(n;t)] \\ \Delta Q_{Peltier}(n;t) &= \Delta K_{Peltier}(n)I(t) \\ \Delta Q_{Couple}(n;t) &= \Delta K_{couple}(n)\theta(n;t). \end{aligned} \quad (7.3)$$

In the step-equation (7.2), the Peltier heating/cooling and the conductance through the thermocouple are regarded as point sources in the equation.

7. 3. Thermal system in SJTC

7. 3. 1. Modeling of SJTC

The numerical simulation was performed on the simplified mathematical model of a SJTC (**figure 7.1**). The temperature distribution along the heater and the support-leads of the SJTC was calculated regarding the SJTC as a one-dimensional thermal system. The heater and the two support-leads were divided into small segments. The glass-base is taken as the heat-sink of the system. The Joule heat generated in the heater is conducted down to the heat sink through the support-leads and the thermocouple.

The dimensional parameters and the thermoelectric constants which have been used in this model are;

- (1) Cross-sectional area
 - $A_{Heater} = 3.1 \times 10^{-10} \text{ m}^2$
 - $A_{Support} = 4.9 \times 10^{-8} \text{ m}^2$
 - $A_{Couple} = 5.0 \times 10^{-11} \text{ m}^2$

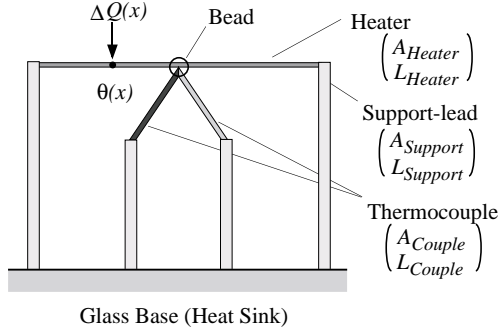


Figure 7.1 One-dimensional model of the heater and the support leads for the calculation of the temperature distribution along the heater of an SJTC.

(2) Length

$$L_{\text{Heater}} = 5.0 \times 10^{-3} \text{ m}$$

$$L_{\text{Support}} = 10.0 \times 10^{-3} \text{ m}$$

$$L_{\text{Couple}} = 10.0 \times 10^{-3} \text{ m}$$

(3) Electric Resistivity

$$\rho_{\text{Heater}} = 108.0 \times 10^{-8} \Omega \text{ m}$$

$$\rho_{\text{Support}} = 27.0 \times 10^{-8} \Omega \text{ m}$$

(4) Thermal Conductivity

$$k_{\text{Heater}} = 17.0 \text{ W m}^{-1} \text{ K}^{-1}$$

$$k_{\text{Support}} = 31.0 \text{ W m}^{-1} \text{ K}^{-1}$$

$$k_{\text{Couple}} = 380.0 \text{ W m}^{-1} \text{ K}^{-1}$$

(5) Thomson Coefficient

$$\sigma_{\text{Heater}} = -2.0 \times 10^{-6} \text{ V K}^{-1}$$

(6) Thermal Capacitance per volume

$$C_{\text{Heater}} = 3.6 \times 10^6 \text{ J m}^{-3} \text{ K}^{-1}$$

$$C_{\text{Support}} = 2.9 \times 10^6 \text{ J m}^{-3} \text{ K}^{-1}$$

The temperature distribution $\theta(x)$ was calculated for current level of 10 mA. The Thomson effect at support-leads is neglected in this model, and the Thomson coefficient of the heater is assumed to be independent on the temperature.

Using the values defined above, the equation (6.22) which represent the basic relationship between the characteristic lengths λ_2 and the characteristic time constant τ are evaluated to be

$$\begin{aligned} \lambda_2[\text{heater}] &= 4.8 \times 10^{-3} \sqrt{\tau} \text{ m} \\ \lambda_2[\text{support}] &= 3.2 \times 10^{-3} \sqrt{\tau} \text{ m}. \end{aligned} \quad (7.4)$$

7.3.2. Effectiveness of the thermoelectric effect

The thermal resistance of the heater, support lead, and the thermocouple for the SJTC are calculated as

$$\begin{aligned} Z_{\text{Heater}} &= L_{\text{Heater}} / A_{\text{Heater}} k_{\text{Heater}} = 9.5 \times 10^5 \text{ K/W} \\ Z_{\text{Support}} &= L_{\text{Support}} / A_{\text{Support}} k_{\text{Support}} = 6.6 \times 10^3 \text{ K/W} \\ Z_{\text{Couple}} &= L_{\text{Couple}} / A_{\text{Couple}} k_{\text{Couple}} = 5 \times 10^5 \text{ K/W} \end{aligned} \quad (7.5)$$

In this model, the heat generated by electric resistance and thermoelectric effects are absorbed by the heat sink through the three paths, i.e., through the two support leads and through the thermocouple. The heat generated near the bead is more effective than the heating near the support lead for raising the temperature at the bead. The effectiveness of the heating is given by a quantity $\Delta\theta_{\text{Couple}}/Z_{\text{Total}}\Delta Q$ as a function of the distance x from the bead.

$$\frac{\Delta\theta_{\text{Couple}}}{Z_{\text{Total}}\Delta Q} = 1 - \frac{2x}{L_{\text{Heater}}} \times \frac{Z_{\text{Heater}}}{2Z_{\text{Support}} + Z_{\text{Heater}}} \quad (7.6)$$

where Z_{Total} represents the total thermal resistance from the bead to the base:

$$\frac{1}{Z_{\text{Total}}} \equiv \frac{1}{Z_{\text{Couple}}} + \frac{4}{2Z_{\text{Support}} + Z_{\text{Heater}}}. \quad (7.7)$$

The effectiveness of local heating is illustrated in **figure 7.2**. The formula (7.6) can also be applied to the second-order thermoelectric heating/cooling which do not change polarity with the reversal of current. For the heating at the heater/support-lead junction ($x=L_{\text{Heater}}/2$), change in the temperature at the bead is evaluated to be $\approx 2Z_{\text{Support}}/Z_{\text{Heater}}$. In the case of the SJTC, the thermoelectric effect near the bead is calculated to be 70 times more effective than the effect near the heater/support junction.

7.3.3. Joule heating

The steady-state temperature distribution along the heater due to the joule heating was obtained using the simplified model of the SJTC. In the step-by-step calculation (7.2), the heater and the support leads are divided to 99 segments, as shown in **figure 7.3**.

The heater is divided to 79 segments (#11 to #89), and the two support-leads are divided to 10 segments each (#1 to #10 and #90 to #99). The segments #10 and #90 represent the heater/support-lead junctions, and the segment #50 represents the center of the heater where the heater is connected

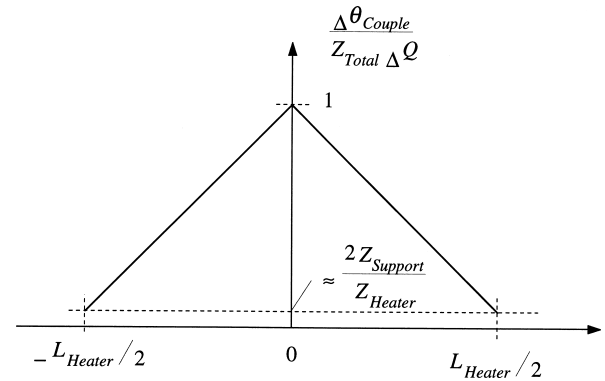


Figure 7.2 The effectiveness of local heating due to the second-order thermoelectric heating/cooling. In the case of the SJTC, the thermoelectric effect near the bead is 70 times more effective than the effect at the heater/support junction.

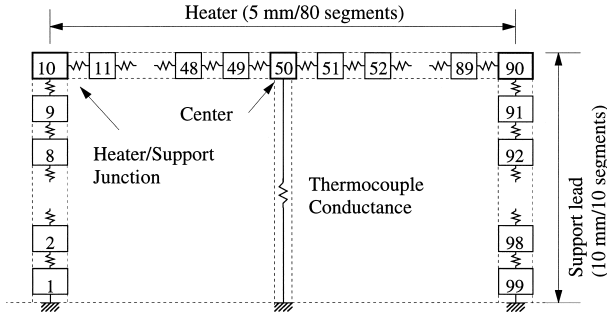


Figure 7.3 Segmented model of the heater and the support leads. The segment #11 to #89 represents the heater, and the segments #1 to #10 and #90 to #99 represents the two support-leads. The segment #50 (center) represent position of a bead. The segment #1 and #99 are connected to the heat sink.

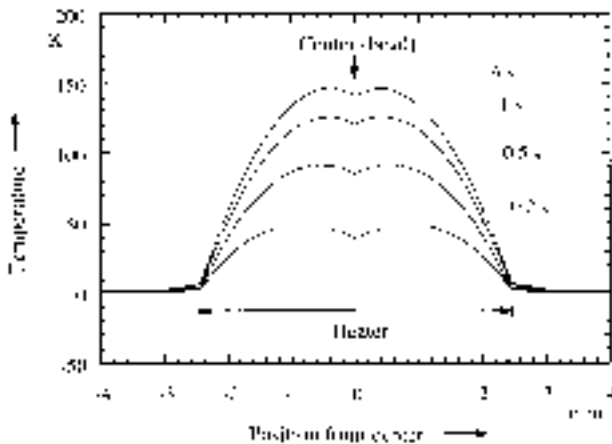


Figure 7.4 The calculated temperature distribution along the heater. The dip at the bead is due to conduction of the heat through the thermocouple.

to the thermocouple by a bead. The segment #1 and #99 are connected to the heat sink, and define the reference point ($\theta_1 = \theta_{99} = 0$).

The step-by-step calculation was performed with standard time-increment (Δt) of 0.2 ms. The calculated temperature distribution along the heater is shown in **figure 7.4**. The temperature distribution reaches its steady-state condition in several seconds. The dip at the bead is due to conduction of the heat through the thermocouple.

In the case of FRDC-DC difference measurement, the rectangular waveform produces constant power. The temperature distribution is always kept at its steady-state condition regardless of the switching frequency f_{sw} .

The development of the temperature distribution with time is shown in **figure 7.5**. The upper and lower curves represent the temperature rise at the bead and at the heater/support junction respectively. The solid curve represents the result of simulation and the dotted curve represents exponential curve fitted to the solid line. From the exponential curve, the time constants for the heater and for the support leads are evaluated to be 0.51 s and 2.15 s, respectively. The characteristic length of the heater is evaluated to be 6.8 mm ($2\lambda_1$)

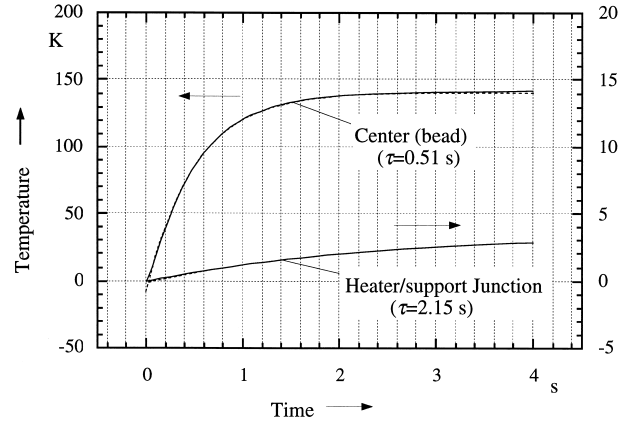


Figure 7.5 The development of the joule heat-up with time. The upper and lower curves represent the temperature rise at the bead and at the heater/support junction respectively. The solid curve represents the result of simulation and the dotted curve represents exponential curve fitted to the solid line.

and 3.3 mm ($2\lambda_2$) in fair agreement with the actual length.

7. 4. Thermoelectric effects in SJTC

In this chapter, the following four different origins of the thermoelectric effects are investigated using the simulation.

- (a) The second-order Thomson effect along the heater.
- (b) Peltier effect at the heater/support lead junctions.
- (c) Localized Thomson effect in the vicinity of the bead.
- (d) Peltier effect in the vicinity of the bead.

Since the establishment of the thermal ac-dc transfer standard in 1960s, the thermoelectric effects have been regarded as the main source of the ac-dc difference. The influence of the Thomson and the Peltier effects on the ac-dc difference has been investigated in detail by Hermach[6], Widdis[7] and Inglis[10, 11]. Though the thermoelectric effects near the bead have not been investigated in their analysis, thermoelectric time constants of smaller than 0.1 s is frequently observed in the FRDC-DC difference measurements. Hence the localized Thomson and the Peltier effect were included in the simulation.

7. 4. 1. Procedure of simulation

The amount of non-joule heating caused by the Thomson and the Peltier effects are more than two orders of magnitude smaller than that of the joule-heating. Hence the thermoelectric effects can be treated as a perturbation in the simulation. The procedure for determining the frequency dependence of FRDC-DC difference due to thermoelectric effects is as follows.

- [1] Calculate the steady-state temperature distribution $\theta_0(x)$ due to Joule heating.
- [2] Calculate the change in the temperature distribution $\Delta\theta_{1st}(dc;x)$ due to the first-order thermoelectric effects in the dc mode.
- [3] Calculate the change in the temperature distribution

$\Delta\theta_{2nd}(dc;x)$ due to the second-order thermoelectric effects in the dc mode.

- [4] Calculate the change in the temperature distribution $\Delta\theta_{1st}(f_{SW};x,t)$ due to the first-order thermoelectric effects in the FRDC mode for one period of reversal.
- [5] Calculate the change in the temperature distribution $\Delta\theta_{2nd}(f_{SW};x,t)$ due to the second-order thermoelectric effects in the FRDC mode for one period of reversal.
- [6] Calculate the averaged temperature change at the bead $\langle\Delta\theta_{2nd}(f_{SW};0,t)\rangle$ due to the thermoelectric effects in the FRDC mode for one period of reversal.

The procedure [1] has been performed in the section 7.3.3. By the repetition of the procedure [4] to [6] while changing the switching frequency f_{SW} , the frequency dependence of FRDC-DC difference is obtained using the following formula:

$$\delta_{FRDC-DC}(f_{SW}) = -\frac{\langle\Delta\theta_{2nd}(f_{SW};0,t)\rangle - \Delta\theta_{2nd}(dc;0)}{2\theta_0(0)} \quad (7.8)$$

7.4.2. Thomson effect of uniform heater

The second-order Thomson effect along the heater is the main source of the ac-dc difference. The temperature distribution $\Delta\theta_{1st}(f_{SW};x,t)$ due to the first-order Thomson effect was evaluated using the step-equation (7.2) for one period of the FRDC waveform. The result of the simulation is shown in **figure 7.6**. The curves represent the temperature distribution along the heater immediately before the reversal of the current. The Thomson coefficient is assumed to be uniform over the length of the heater. At reversing frequencies less than 1 Hz, the temperature distribution approaches that of dc. For the higher reversing frequencies, the first-order effect does not have enough time to buildup the temperature distributions and, therefore, it is totally suppressed at frequencies higher than 100 Hz.

Since the temperature distribution has anti-symmetry, the

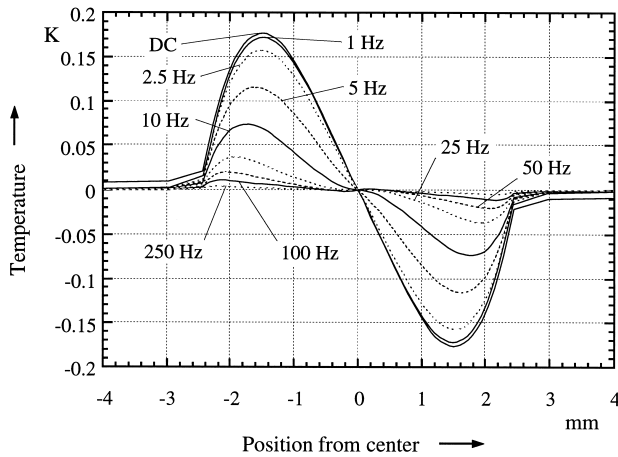


Figure 7.6 The temperature distribution due to the first-order Thomson effects immediately before the reversal of the current.

center of the heater ($x=0$) may be recognized as the imaginary heat-sink. In this case, the thermoelectric effect has a characteristic length equal to the half-length of the heater.

Since the Thomson effect produces the first-order temperature distribution of the order of 0.1 K, a non-negligible amount of the second-order Thomson heating/cooling is generated along the heater of the SJTC. **Figure 7.7** shows the calculated second-order Thomson heating/cooling in the vicinity of the bead. The exponential behavior of the second-order Thomson heating/cooling confirms the adequacy of the assumption used in the derivation of formula (6.15) deduced in chapter 6;

$$\delta_{FRDC-DC} = \delta_{TE} \left(\frac{2\tau_{TE}}{T_{SW}} \right) \tanh \left(\frac{T_{SW}}{2\tau_{TE}} \right) \quad (6.15)$$

In the case of the reversing frequency of 2.5 Hz, which is slightly below the characteristic frequency, the heating- and cooling-power compensate each other and the average power is much smaller than that for 0.25 Hz.

Figure 7.8 shows the result of the evaluated FRDC-DC

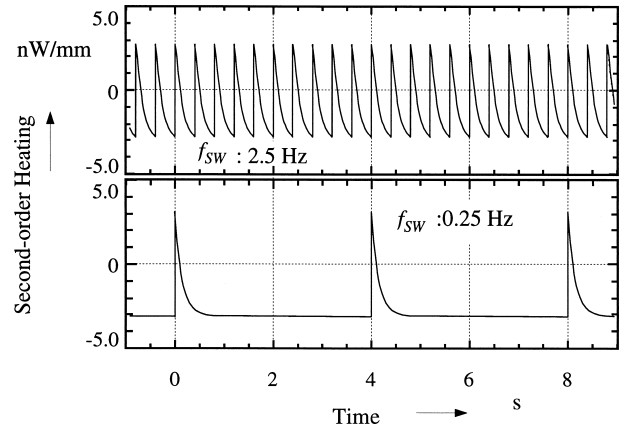


Figure 7.7 Second-order Thomson heating and cooling. The upper graph is for the reversing-frequency of 2.5 Hz, and lower graph is for 0.25 Hz.

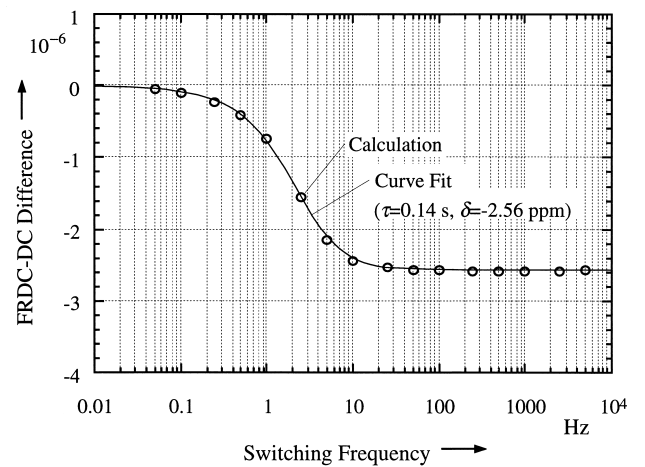


Figure 7.8 Simulated FRDC-DC difference $\delta_{FRDC-DC}(f_{SW})$ for frequency range between 0.05 Hz to 5 kHz. The thermoelectric time constant of the heater is evaluated to be 0.14 s by the curve-fitting.

difference $\delta_{FRDC-DC}(f_{SW})$ for frequency range between 0.05 Hz to 5 kHz. From the frequency dependence of $\delta_{FRDC-DC}(f_{SW})$, the thermoelectric time constant of the heater is evaluated to be 0.14 s, using the formula (6.15). On the other hand, by the direct curve-fitting of the data shown in figure 7.7 to an exponential response function, the time-constant of the second-order Thomson effect is evaluated to be 0.15 s. The good agreement in the two numbers confirms the adequacy of the simple exponential model assumed in the derivation of the formula (6.15).

Using the formula (7.4), the characteristic length of the heater and the support lead are estimated to be 1.7 mm ($2\lambda_2$), in agreement with the half-length of the heater (2.5 mm).

In the case of uniformly distributed Thomson effect, the ac-dc difference was evaluated by Widdis[7] as:

$$\delta_{ac-dc} = -\frac{1}{12} \frac{\sigma^2 \theta_0}{\rho k} \quad (7.9)$$

where the symbols σ , θ_0 , ρ , and k represent the Thomson coefficients, mid-point temperature-rise, electric resistivity, and the thermal conductivity of the heater. Using the value defined in the section 7.3.1 for the parameters, the equation (7.9) is evaluated to be -2.58 ppm. In the case of simulated FRDC-DC difference measurement, the thermal transfer difference is evaluated to be -2.56 ppm, in good agreement with the analytical value.

Recently manufactured SJTCs, such as SS283 from Best Technology, use Evanohm for the heater material. In this case, Thomson coefficients are nearly ten times smaller than the value used in this simulation. As will be described in the next chapter, these new SJTCs exhibit thermoelectric transfer differences smaller than 1 ppm.

7. 4. 3. Peltier effect at heater/support junction

Another well-known source of the ac-dc difference is the Peltier effect at the heater/support-lead junctions where different material is joined. The Peltier effect causes a linear temperature gradient across the heater, and result in uniformly distributed second-order Thomson heating/cooling along the heater.

The temperature distribution $\Delta\theta_{1st}(f_{SW};x,t)$ due to the Peltier effect is shown in **figure 7.9**. With the Peltier coefficient of 2.2 mV, heating/cooling power of $\pm 22 \mu\text{W}$ is generated at the junctions, resulting in the linear $\pm 0.1 \text{ K}$ temperature gradient across the heater. Since the thermal capacitance of the support lead is 80 times as large as that of the heater, changes in the temperature at the heater/support junction are mainly determined by the time constant of the support lead. Hence the thermoelectric effect is expected to have a characteristic length equal to the size of the support lead.

Figure 7.10 shows the result of the evaluated FRDC-DC difference $\delta_{FRDC-DC}(f_{SW})$. From the frequency dependence of $\delta_{FRDC-DC}(f_{SW})$, the thermoelectric time constant of the Peltier effect is evaluated to be 1.9 s, in good agreement with the time constant of the joule heating at the heater/support junction.

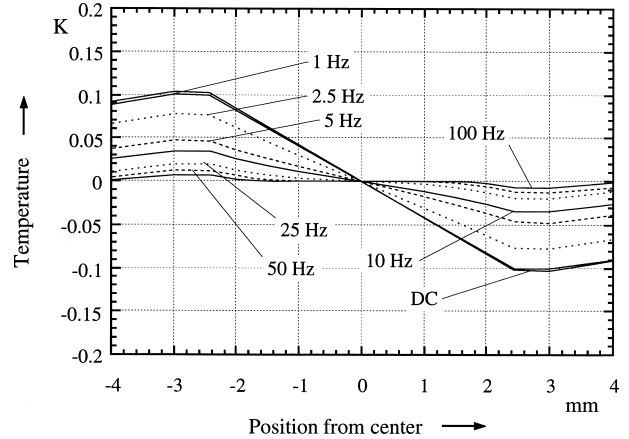


Figure 7.9 The temperature distribution due to the first-order Peltier effects immediately before the reversal of the current. The Peltier coefficient at the junctions produces linear temperature gradient across the heater.

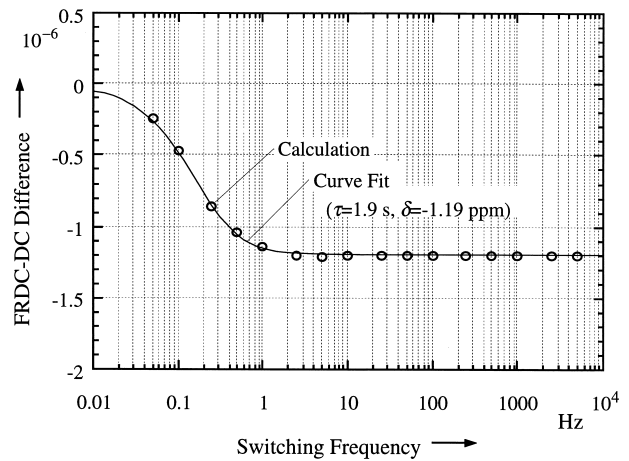


Figure 7.10 Simulated FRDC-DC difference $\delta_{FRDC-DC}(f_{SW})$ for frequency range between 0.05 Hz to 5 kHz. The thermoelectric time constant of the Peltier effect is evaluated to be 1.9 s by the curve-fitting.

The ac-dc difference due to the Peltier effect at the heater/support junction is also been given by Widdis[7] as,

$$\delta_{ac-dc} = \frac{\sigma \delta\theta}{V_h} \quad (7.10)$$

where the symbols $\delta\theta$ and V_h represents the temperature difference and voltage drop across the heater.

The temperature difference $\delta\theta$ was obtained by the first-order distribution to be 0.1 K. Using the value defined in the section 7.3.1, the equation (7.10) is evaluated to be -1.21 ppm. The value is in good agreement with the value (-1.19 ppm) obtained by the simulated FRDC-DC difference measurement.

7. 4. 4. Thomson effect in the vicinity of the bead

In the conventional design of the SJTC elements, the glass-beads which thermally connects the heater and thermocouple are formed by flaming. In the process of flaming, the heater near the bead is also exposed to the flame. Hence

it is plausible that the thermoelectric property of the heater-material is locally deteriorated in the vicinity of bead. In this sub-section, the effect of local change in the Thomson coefficient is analyzed. In the simulation, it is assumed that the Thomson coefficient is enhanced in the range of ± 0.1 mm from the bead. To be more specific, the Thomson coefficient of the three segments #49 to #51 in figure 7.3 is modified from $-2.0 \mu\text{V/K}$ to $-20 \mu\text{V/K}$. The other conditions are the same as the calculation of the Thomson effect for uniform heater as described in section 7.4.1.

The temperature distribution $\Delta\theta_{1st}(f_{SW};x,t)$ is shown in **figure 7.11**. The over-all shape is quite similar to the case of the uniform heater, except that local structure in the temperature distribution is observed near the bead.

Figure 7.12 shows the result of the simulated FRDC-DC

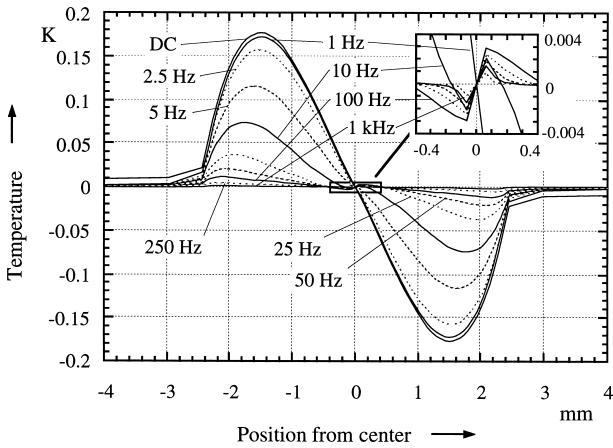


Figure 7.11 The temperature distribution due to the first-order Thomson effects immediately before the reversal of the current. The local structure in the temperature distribution is observed near the bead.

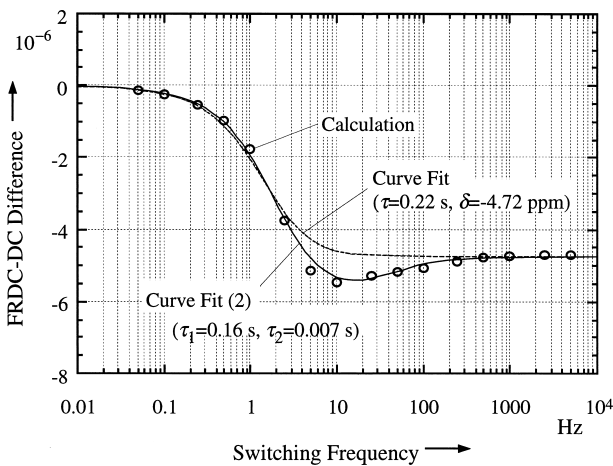


Figure 7.12 Simulated FRDC-DC difference $\delta_{FRDC-DC}(f_{SW})$ for frequency range between 0.05 Hz to 5 kHz. The frequency dependence is characterized by two thermoelectric time constants of 0.16 s and 0.007 s.

difference $\delta_{FRDC-DC}(f_{SW})$. The frequency dependence of $\delta_{FRDC-DC}(f_{SW})$ is characterized by two thermoelectric time constants of 0.16 s and 0.007 s. The former time constant agrees with the time constant of 0.14 s for the uniform heater. Using the formula (7.4), the characteristic length of the local Thomson effect is estimated to be 0.4 mm ($2\lambda_2$), which is similar to the size of the region (0.25 mm) in which the Thomson effect is enhanced.

7.4.5. Peltier effect in the vicinity of the bead

If there is a local change in the property of the heater-material, the Peltier heating or cooling power can be generated at the boundary. In this sub-section, the Peltier effect in the vicinity of the bead is considered. In the simulation, it is assumed that the heating-spot and cooling-spot are separated 0.25 mm. To be more specific, the segments #48 and #52 in figure 7.3 have the Peltier coefficient of -0.2 mV and $+0.2$ mV, respectively. The other conditions are the same as the case of the Thomson effect for uniform heater as described in section 7.4.1. The Peltier effects at heater/support junctions are also neglected in this calculation. The local change in the Thomson coefficient will be included in the next calculation.

The temperature distribution $\Delta\theta_{1st}(f_{SW};x,t)$ is shown in **figure 7.13**. The sharp anti-symmetric peaks near the bead represent the pair of Peltier heating- and cooling- spots. The temperature gradient near the bead is 0.36 K/mm, which is more than two times steeper than that for the first-order Thomson effect for the uniform heater.

Figure 7.14 shows the result of the simulated FRDC-DC difference $\delta_{FRDC-DC}(f_{SW})$. In spite of large temperature gradient in the vicinity the bead, the thermal transfer difference is five-times smaller than the case of the Thomson effect for uniform heater. The ineffectiveness of the local Peltier effect is due to the fact that the Peltier effect produces both

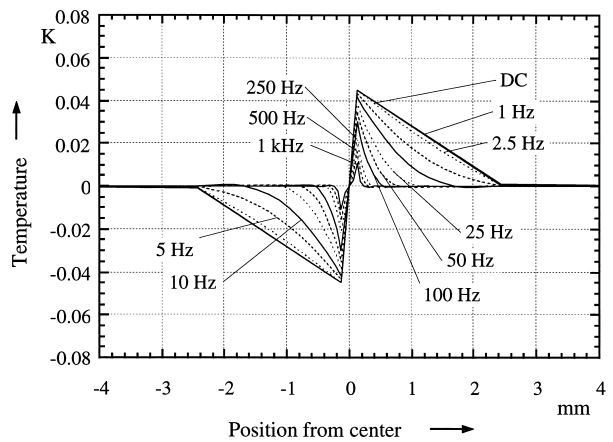


Figure 7.13 The temperature distribution due to the localized Peltier effects immediately before the reversal of the current. The sharp anti-symmetric peaks near the bead represent the pair of Peltier heating- and cooling- spots.

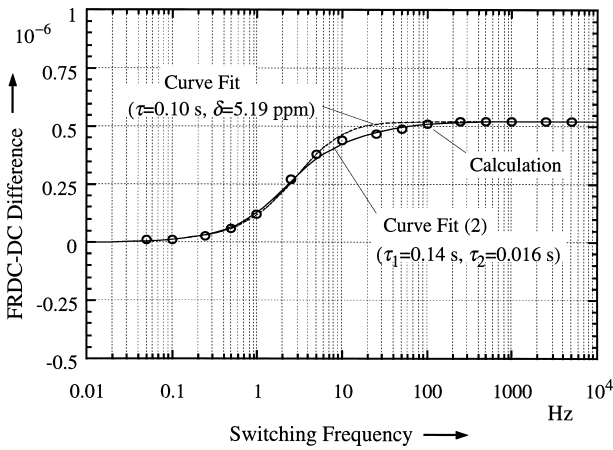


Figure 7.14 Simulated FRDC-DC difference $\delta_{FRDC-DC}(f_{SW})$ for frequency range between 0.05 Hz to 5 kHz. The frequency dependence of $\delta_{FRDC-DC}(f_{SW})$ is characterized by the two thermoelectric time constants of 0.14 s and 0.016 s.

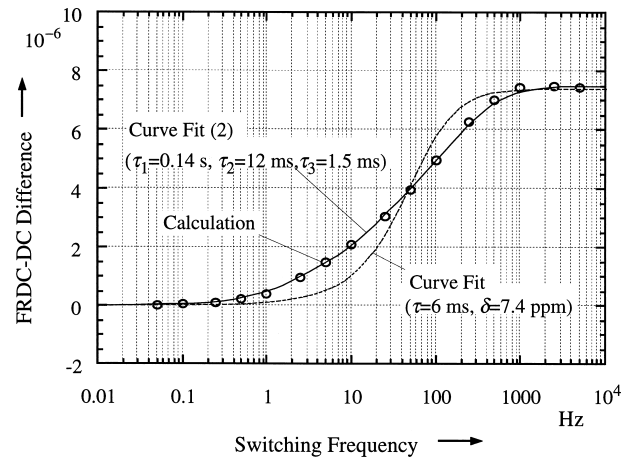


Figure 7.15 Simulated FRDC-DC difference $\delta_{FRDC-DC}(f_{SW})$ for frequency range between 0.05 Hz to 5 kHz. Three time constants were required to fit the frequency dependence by the formula; 0.14 s, 0.012 s and 0.0015 s.

positive and negative temperature gradients. The Thomson cooling in the positive-gradient region within the boundary is tend to be canceled by the negative-gradient region outside the boundary.

The frequency dependence of $\delta_{FRDC-DC}(f_{SW})$ is characterized by the two thermoelectric time constant of 0.14 s and 0.016 s. The former time constant agrees with the time constant of 0.14 s for the uniform heater. The shorter time constant, which reflects the local Peltier effects, gives relatively small contribution to the thermal transfer difference. Using the formula (7.4), the characteristic length of the local Peltier effect is estimated to be 0.6 mm ($2\lambda_2$).

7. 4. 6. Combination of local Thomson and Peltier effects

In the analysis performed in section 7.4.4 and 7.4.5, the effects of local change in the Thomson coefficient and the change in the Peltier coefficient have been analyzed separately. The more realistic assumption is that both the Thomson coefficient and the Peltier coefficient are altered locally as the consequence of the flaming. In this model, the measurement condition is the combination of that given in 7.4.4 and 7.4.5:

- (a) The Thomson coefficient is enhanced from $-2.0 \mu\text{V}/\text{K}$ to $-20 \mu\text{V}/\text{K}$ in the range of ± 0.13 mm from the bead.
- (b) A pair of heating/cooling-spot separated 0.25 mm is created with Peltier coefficient of ± 0.2 mV.

The result of the evaluated FRDC-DC difference $\delta_{FRDC-DC}(f_{SW})$ is shown in **figure 7.15**. Probably due to the complex structure of the thermal property of the heater, three time constants were required to fit the frequency dependence by the formula. One of the time constant τ_1 was fixed to 0.14 s, and the other two time constants were evaluated by least-square fitting to be $\tau_2=0.012$ s and $\tau_3=0.0015$ s.

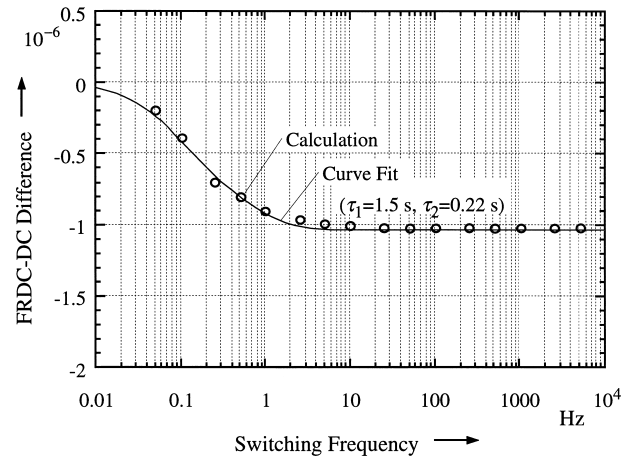


Figure 7.16 Simulated FRDC-DC difference $\delta_{FRDC-DC}(f_{SW})$ for frequency range between 0.05 Hz to 5 kHz. The frequency dependence of $\delta_{FRDC-DC}(f_{SW})$ is characterized by the two thermoelectric time constants of 0.22 s and 1.5 s.

7. 4. 7 Seebeck effect at heater/support junction

The Peltier effect at the heater/support-lead junctions causes a linear temperature gradient across the heater. The difference in the temperature between the two heater/support junctions produces a net thermal EMF in the input circuit due to the Seebeck effect. As will be analyzed in detail in section 8.3.2, the thermal EMF leads to a thermoelectric transfer difference which occurs only in the voltage mode.

Figure 7.16 shows the result of the evaluated FRDC-DC difference $\delta_{FRDC-DC}(f_{SW})$. The frequency dependence of $\delta_{FRDC-DC}(f_{SW})$ is characterized by two thermoelectric time constants of 0.22 s and 1.5 s. The former time constant agrees with that of the Thomson effect described in section 7.4.2, while the latter agrees with that of the Peltier effect described in section 7.4.3. Hence the two time constants seem to correspond to the time constant of the heater and the support-leads, respectively.

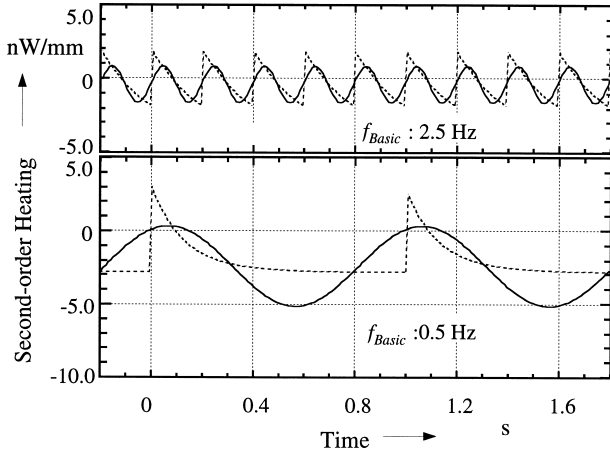


Figure 7.17 Development of the second-order Thomson heating/cooling with time. The solid lines represent the response to the sinusoidal waveform, and the dotted curves represent the response to rectangular waveform. The upper graph is for the basic-frequency of 2.5 Hz (5 Hz switching frequency for FRDC waveform), and lower graph is for 0.5 Hz.

7.5 Excitation by sinusoidal waveform

The step equation (7.2) may also be used to determine the response of the thermal system to the excitation by sinusoidal waveform. In this case, frequency dependence of the ac-dc transfer difference due to the thermoelectric effect can be evaluated.

Figure 7.17 shows the development of the second-order Thomson heating/cooling with time. The solid lines represent the response to the sinusoidal waveform, and the dotted curves represent the response to rectangular waveform. The upper graph is for the basic-frequency of 2.5 Hz (5 Hz switching frequency for FRDC waveform), and lower graph is for 0.5 Hz. While there is a noticeable difference in the response to rectangular and sinusoidal waveform at lower frequencies, the difference becomes smaller at higher frequencies.

Calculated ac-dc difference and the FRDC-DC difference contributed from the second-order Thomson effect are shown in **figure 7.18**. The peak-to-peak amplitude of the thermal

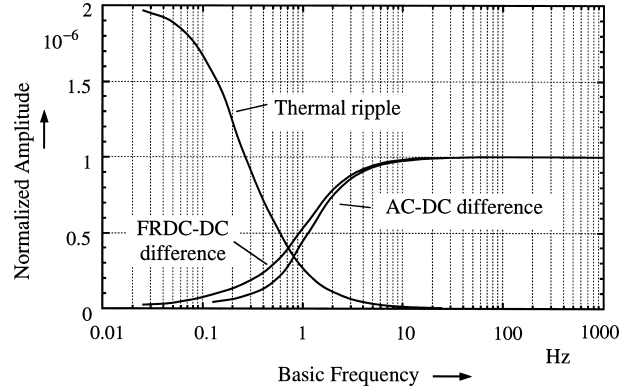


Figure 7.18 Calculated ac-dc difference and the FRDC-DC difference contributed from the second-order Thomson effect. The peak-to-peak amplitude of the thermal ripple for the sinusoidal excitation is also shown in the figure. All the curve is normalized relative to the value for the steady-state DC.

ripple for the sinusoidal excitation is also shown in the figure. All the curve is normalized relative to the value for the steady-state DC. The frequency dependence of the ac-dc difference due to the Thomson effect is quite similar to that of the FRDC-DC difference, as expected.

Usually the effect of thermal ripple is one or two orders of magnitude larger than the thermoelectric effect. Hence the frequency-dependent part of the of the thermoelectric effect is dominated by the thermal ripple, and may not be observed in the actual ac-dc transfer difference measurement. On the other hand, if the thermoelectric time constant is much smaller than the time constant of the joule heating, as in the case of the local Thomson or Peltier effect, It may be possible to observe the effect in the ac-dc difference measurement.

7.6 Summary

The thermoelectric effects of different origins are analyzed using the numerical simulation on an SJTC. Time-constants determined by the simulated FRDC-DC difference measurement are summarized in **table 7.1**. The first two

Table 7.1 Time constants determined by simulated FRDC-DC difference measurement.

Effect (localization)	Time constants (s)		Characteristic length (mm)	
	1st	2nd	1st	2nd
Joule (heater)	0.51		5.0	
Joule (junction)	2.15		10.0	
Thomson (heater)	0.14		2.5	
Peltier (junction)	1.9		10.0	
Peltier (EMF)	1.5	0.22	10.0	2.5
Thomson (local)	0.16	0.007	2.5	0.25
Peltier (local)	0.14	0.016	2.5	0.25

entries in the table represent the time-constants of Joule heating evaluated for the heater and the support-lead. Since the thermal capacitance of the support-lead is two orders of magnitude larger than that of the heater, changes in the temperature at the heater/support junctions are mainly determined by the time-constant of the support-lead. In the case of the Thomson effect, the first-order temperature distribution has asymmetry, as was shown in figure 7.6. Since the center of the heater may be recognized as the imaginary heat-sink, half-length of the heater is taken as the characteristic length for the Thomson effect.

The relationship between the characteristic scale and the characteristic time-constants of the thermoelectric effects are plotted in **figure 7.19**. The plotted data show the result of the numerical simulation on the different origins of thermoelectric effects. The solid lines represent the simple theoretical formula (7.4) predicted for a one-dimensional thermal system. The upper part of the line represents the support-lead, the lower part of the line represents the heater. The good agreements suggest that the formula presents a fundamental relationship between the characteristic length and the characteristic time-constants of the thermoelectric effects. Hence, the thermoelectric time-constants determined by the FRDC-DC measurement give us an important insight into the location and the origin of the thermoelectric effects.

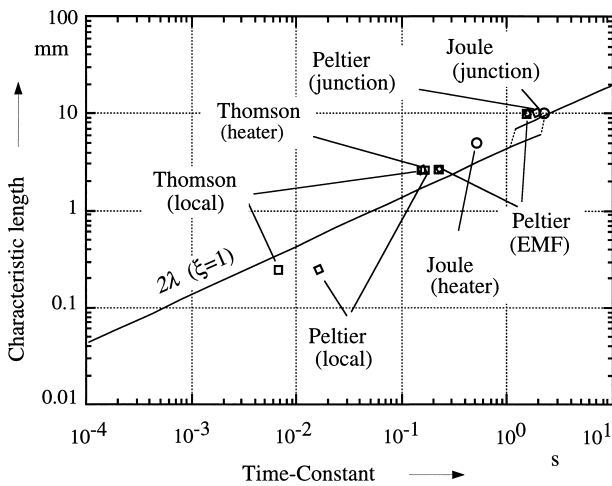


Figure 7.19 Relationship between thermoelectric time-constants and the characteristic lengths associated with it. The solid lines represent the simple theoretical formula for the heater (lower part) and support-lead (upper part), respectively.